Assembly processes of bacterial and fungal communities in metal(loid)s smelter soil

Miaomiao Li, Jun Yao, Geoffrey Sunahara, Robert Duran, Bang Liu, Ying Cao, Hao Li, Wancheng Pang, Houquan Liu, Shun Jiang, et al.

Assembly processes of bacterial and fungal communities in metal(loid)s smelter soil

Miaomiao Li[a], Jun Yao[a*], Geoffrey Sunahara[a,b], Robert Duran[c], Bang Liu[a], Ying Cao[a], Hao Li[a], Wancheng Pang[a], Houquan Liu[a], Shun Jiang[a], Junjie Zhu[a], Qinghua Zhang[d]

[a] Science and Engineering, China University of Geosciences (Beijing), 29 Xueyuan Road, Haidian District, Beijing 100083, China

[b] Department of Natural Resource Sciences, McGill University, 21111 Lakeshore Drive, Ste-Anne-de-Bellevue, Quebec, H9X 3V9, Canada

[c] Universite de Pau et des Pays de l'Adour, UPPA/E2S, IPREM CNRS 5254, Pau, France

[d] College of Bioscience and Engineering, Jiangxi Agricultural University, Nanchang 330045, PR China

* Corresponding author:

Jun Yao (E-mail: yaojun@cugb.edu.cn)

School of Water Resource and Environment, Research Center of Environmental Science and Engineering, China University of Geosciences (Beijing), 29 Xueyuan Road, Haidian District, 100083, Beijing, China

Abstract

The assembly processes of microbial communities governing the metal(loid)s biogeochemical cycles at smelters are yet to be solved. Here, a systematic investigation combines geochemical characterization, co-occurrence patterns, and assembly mechanisms of bacterial and fungal communities inhabiting soil around an abandoned arsenic smelter. *Acidobacteriot*a, *Actinobacteriota*, *Chloroflexi*, and *Pseudomonadota* were dominant in the bacterial communities, whereas *Ascomycota* and *Basidiomycota* dominated the fungal communities. The random forest model indicated the bioavailable fractions of Fe were the main positive factor driving the beta diversity of bacterial communities (9.58%) and the negative impact of total N on fungal communities (8.09%). The microbial-contaminant interactions demonstrate the positive impact of the bioavailable fractions of certain metal(loid)s on bacteria (*Comamonadaceae* and *Rhodocyclaceae*) and fungi (*Meruliaceae and Pleosporaceae*). The fungal co-occurrence networks exhibited higher connectivity and complexity than the bacterial networks. Interestingly, positive links dominated all networks. The keystone taxa were identified in bacterial (including the family *Diplorickettsiaceae*, *norank_o__Candidatus_Woesebacteria*, *norank_o__norank_c__AT-s3-28*, *norank_o__norank_c__bacteriap25*, and *Phycisphaeraceae*) and fungal (including *Biatriosporaceae*, *Ganodermataceae*, *Peniophoraceae*, *Phaeosphaeriaceae*, *Polyporaceae*, *Teichosporaceae*, *Trichomeriaceae*, *Wrightoporiaceae*, and *Xylariaceae*) communities. Meanwhile, community assembly analysis revealed that deterministic processes (especially variable selection) dominated the microbial community assemblies, which were highly impacted by the pH, total N, and total and bioavailable metal(loid) content. This study

provides a deeper insight into the organization of microbial communities in response to long-term metal(loid)s pollution and helpful information to develop bioremediation strategies for the mitigation of metal(loid)s-polluted soils.

Keywords: Metal(loid)s, Bacterial and fungal community, Co-occurrence pattern, Assembly mechanism

1. Introduction

More than 10 million sites present metal(loid)s polluted soils worldwide, being a major concern for society and the scientific community (Fei et al., 2019; Zhang et al., 2020; Xu et al., 2021a). Metal smelting activity is considered one of the main anthropogenic sources of metal(loid)s pollution in soil (Yun et al., 2018). Smelting operations generate large amounts of hazardous solid waste (e.g., smelting slag, combustion residues, and mine tailings) that are deposited near the smelters (Xu et al., 2021a; Liu et al., 2022a). Thus, the dispersion of smelter waste can affect the stability of surrounding ecosystems causing important ecological disturbances (Zhang et al., 2022b). The presence of metal(loid)s can decrease the soil microbial biomass, as well as disrupt the composition and function of soil microbial communities (Park et al., 2021). To date, most studies have investigated the ecological processes of microbial communities under metal(loid)s pressure, usually focusing on only one microbial domain (Liu et al., 2021; Park et al., 2021; Liu et al., 2022a; Zhang et al., 2022c). In addition to bacteria, fungi can play vital roles in soil, including biogeochemical cycling of metal(loid) elements, decomposition of organic matter, and maintenance of ecosystem stability and productivity (Wang et al., 2022b; Zhang et al., 2022c). However, the simultaneous exploration of the responses of bacterial and fungal communities to long-term metal(loid)s contamination in smelting environments has been little studied.

Co-occurrence network analysis has proved to be an efficient tool to explore the responses of microbial communities to environmental stress (Price et al., 2021). Also, the investigation of microbial interactions is critical to understand the complexity and diversity of microbial communities (Zhou et al., 2020). The co-occurrence, competition, and antagonism

between different microbial compartments can be examined using network analyses based on molecular data (Zhang et al., 2022c). Furthermore, the network topological features can identify the keystone taxa. Although extensive studies have explored the complex microbial interactions in metal(loid)s contaminated environments (Sun et al., 2020; Chun et al., 2021; Liu et al., 2022c), only a few studies have investigated the differences between bacterial and fungal communities from the perspective of co-occurrence patterns under metal(loid)s contamination. Investigating the relative importance of assembly-regulating processes in microbial communities under metal(loid)s exposure can help reveal the adaptive responses of microbial communities to environmental stress (Zhang et al., 2022b), such as bacterial communities living in mining and smelting sites (Liu et al., 2022a). However, there remains a knowledge gap in the microbial community assembly processes, particularly when comparing the ecological assembly process of bacterial and fungal communities under diverse metal(loid)s exposure. Therefore, a holistic approach investigating all the components of the microbial community (prokaryotes and eukaryotes) under long-term metal(loid)s contamination is required for a better understanding of the assembly rules involved in the microbial communities in response to metal(loid)s exposure.

We suspected that bacterial and fungal communities will have similar adaptive responses to long-term metal(loid)s exposure. In the present study, soil samples were collected from the Huilong nonferrous metal smelter, which produced mainly arsenic and arsenic trioxide, and was closed for the past 20 years. Studies were conducted to reveal the differences in adaptive responses between bacterial and fungal communities under metal(loid)s exposure. The objectives of this study were to (1) investigate the effects of selected geochemical properties

on bacterial and fungal communities; (2) characterize the co-occurrence patterns of bacterial and fungal communities, and (3) determine the ecological assembly processes of bacterial and fungal under metal(loid)s exposure.

2. Materials and methods

2.1 Study site description

The study area (111°16′48.64″E, 24°27′48.41″N) has a total area of about 16,617 m^2 and is located at Zhongshan City in Guangxi Province, southwestern China (Fig. 1). The study region was divided into different areas, including site XY (belonging to the original roasting reverberatory furnace production workshop, which was later used by another factory), site YBS (the main production workshop, which was since demolished and leveled to the ground; its topography was changed greatly), and site ZD (consisting mainly of large piles of arsenic-containing waste slag and soot slag from the production plant). The surrounding areas proximal to the Huilong factory were each identified numerically at site Y. The climate in this region is subtropical monsoon with distinct wet and dry seasons. The mean annual precipitation is 1576.7 mm, with 47% precipitation occurring between April and June. The mean annual air temperature is 19.7°C, with 39.8°C maximal (in 2003 and 2007) and -3.7°C minimal (in 1969) temperatures.

2.2 Soil sampling

A total of 18 topsoil samples (10-20 cm) were collected in October 2020 using a sterilized shovel. Three soil samples were taken from the Y site, and five soil samples were taken from XY, YBS, and ZD sites (Fig. 1). Each sample was a composite of five sub-samples (each approximately 500 g from the four corners and the center point of a 4 m ×

4 m quadrat). Large-grain gravel and plant residues were removed during the sampling process. Then these samples were stored in separate polyethylene bags placed on ice and transported immediately to the laboratory. After a preliminary treatment (air-dried and pass through a 10-mm mesh sieve), each composite sample was divided into two aliquots (each approximately 50 g), one for the analysis of soil chemical properties at 4°C, and the other was stored at -80°C for DNA extraction.

2.3 Geochemical measurements

Samples were air-dried at room temperature and passed through a 10-mm mesh sieve. The moisture content (MC) was measured using a published procedure (Dettmann et al., 2021). The soil pH and oxidation-reduction potential (ORP) were determined by suspending soil in distilled water (1:3, solid to water, w/v), shaking for 10 min, and equilibrating for 30 min, before the supernatant was measured using a standard PE-28 pH meter (Mettler Toledo, Shanghai). The electrical conductivity (EC) was determined by a Model DDS-11A conductivity meter (Leici, Shanghai) using soil suspended in distilled water (1:5, w/v) according to a previous study (Aponte et al., 2020). Soil total nitrogen (TN) contents were measured by a Vario MACRO cube elemental analyzer (Elementar, Hanau, Germany). For the total organic carbon (TOC) measurements, 5% HCl was added to digest the carbonates of each soil sample and dried at 105°C, then the TOC was measured using a Shimadzu TOC-L Analyzer (Japan). The sulfates were measured on an ICS-600 ion chromatograph (Thermo, USA). The soil metal(loids)s were first digested with a mixture of aqua regia and HF (5:3, v/v) and then the total metal concentrations (for Al, As, Cd, Cr, Cu, Fe, Mg, Mn, Ni, Pb, Sb, Ti, V, and Zn) were determined by inductively coupled plasma optical emission spectrometry

(ICP-OES, Thermo iCAP 7000 SERIES, USA). In addition, the bioavailable fractions of metals (Kim et al., 2014) were obtained using the modified BCR sequential extraction method according to Zhu et al. (Zhu et al., 2018). Four metal(loid)s fractions were collected and detailed information was consistent with a previous paper (Li et al., 2022b). Here the bioavailable fractions are expressed as "element symbolmetal(loid)s_bio," such as As_bio and Cd_bio, etc. Each sequential digested filtrate was rinsed with distilled water and filtered before ICP-OES analysis. All samples were analyzed in triplicate for the quality of data.

2.4 DNA extraction, amplification, and sequencing

DNA extraction was conducted using the MoBio PowerSoil® DNA isolation kit (MO BIO Laboratories, Carlsbad, CA, USA) according to the manufacturer's instructions. The quality of extracted DNA was evaluated by the NanoDrop 2.0 spectrophotometer (Thermo Fisher Scientific, CA, USA). A Quant-IT Pico Green dsDNA Kit (Invitrogen Molecular Probes Inc, Oregon, USA) was used to examine the final DNA concentration. Primer pairs 515F (GAGCCAGCMGCCGCGGTA) and 806R (GGACTACHVGGGTWTCTAAT) were used to amplify the V4 region of the bacterial 16S rRNA gene. Primer pairs ITS1F (CTTGGTCATTTAGAGGAAGTAA) and ITS2R (GCTGCGTTCTTCATCGATGC) were used to amplify the ITS1 region of the fungal rRNA gene (Liu et al., 2022b). The products of PCR amplification and tag-encoded high-throughput sequencing of the 16S and ITS1 region were conducted by MajorBio (Shanghai, China) using the Illumina platform (Miseq, USA) and quantified by QuantiFluor™-ST microfluorometry (Promega, USA).

The paired-end sequences were merged by the FLASH program based on the default parameters of the equipment (Magoc and Salzberg, 2011). Then the merged sequences were

161 further filtered using QIIME 1.9 for quality, with a size greater than 20 as a threshold of the
162 average Phred quality score. The sequences of chimeric were removed using the USEARCH.
163 The sequences were classified into the operational taxonomic units (OTUs) at a similarity
164 level of 97%, and all singleton OTUs were removed. The representative OTUs of bacteria
165 were classified with the taxonomic information in the SILVA (v138.1) database and the
166 representative OTUs of fungi were classified with the taxonomic information in the UNITE
167 database. Finally, subsampling was performed to normalize the dataset to the sample with the
168 lowest number of reads. The alpha diversity indices (Shannon, Simpson, Chao) were
169 calculated from these samples to evaluate the microbial diversity and richness of bacteria and
170 fungi. The sequence reads of bacteria and fungi obtained here have been submitted to the
171 database of the (National Center of Biotechnology Information) NCBI (Accession No.
172 PRJNA853628 and PRJNA853717, respectively).

173 *2.5 Network construction*

174 The network was adopted to build the co-occurrence patterns of bacterial and fungal
175 communities, exploring the potential relationships among microbes. Initially, the OTU
176 taxonomy file, the relative abundance of OTUs, and the geochemical parameters were
177 assembled for future analysis. Only those genera with the sum of relative abundances higher
178 than 0.005 were kept and the OTUs were filtered that simultaneously appeared in five
179 samples. Subsequently, the Spearman's correlation coefficient analysis ($R > |0.6|$ and $P < 0.05$)
180 was performed to determine the interactions with each of the two genera (Barberan et al.,
181 2012). The correlation matrix was then transformed into the similarity matrix based on the
182 Spearman's correlation coefficient. The global network properties (the average path length,

connectivity, average clustering coefficient, and modularity) were calculated. Among these properties, the average path length is the average distance between two nodes and the average clustering coefficient represents the interconnection of nodes. Connectivity reflects the connection strength between two nodes, and modularity is a measure to divide the network into modules, which is identified as a group of nodes connected more densely than the nodes outside the group (Olesen et al., 2007). The topological properties are commonly used to describe the complex pattern of inter-relationships between OTUs (Wei et al., 2020). Network hubs and connectors are considered the keystone nodes in a network, which play important roles in the stability and resistance of microbial communities. Therefore, the OTUs related to these nodes were defined as keystone species. To investigate the interactions between environmental factors and microorganisms in the samples with different contaminant concentrations, the networks between OTUs and the environmental factors were also constructed. All the networks in this investigation were constructed and analyzed by Gephi 0.9.2 (http://igraph.org).

2.6 Modeling microbial community assembly

Microbial assembly processes are essential for establishing the co-occurrence patterns of community composition within a given ecosystem (Feng et al., 2018). Two complementary mechanisms regulate the assemblages of a microbial community, namely the deterministic (niche-based theory) and stochastic (neutral theory) processes (Zhou and Ning, 2017). The deterministic process emphasizes the dominant role of environmental selection (including biological and non-biological factors) in the microbial assembly process, which largely affects the abundance, composition, and distribution patterns of the microbial communities

(Zhang et al., 2022b). Whereas the stochastic process emphasizes the role of dispersal and ecological drift (Zheng et al., 2021).

The deterministic and stochastic assembly processes of microbial communities observed here were calculated based on the beta nearest taxon index (βNTI) and the Bray-Curtis-based Raup-Click (RC_{bray}). These data were analyzed using the online tool of the Majorbio Cloud Platform (https://cloud.majorbio.com/page/tools/). The value of $|\beta NTI| > 2$ indicates that a deterministic process ($\beta NTI > 2$: variable selection; whereas $\beta NTI < -2$: homogeneous selection) dominates the community assembly process. Otherwise, it indicates the stochastic process ($|\beta NTI| < 2$) dominates the community assembly process (specifically, $|\beta NTI| < 2$ and $RC_{bray} < -0.95$: homogeneous dispersal; $|\beta NTI| < 2$ and $RC_{bray} > 0.95$: dispersal limitation; $|\beta NTI| < 2$ and $|RC_{bray}| < 0.95$: undominated).

2.7 Statistical analyses

The alpha diversity (Shannon, Simpson, or Chao) was estimated using rarified libraries. The Principal Component Analysis (PCoA, beta diversity) was determined by the Bray-Curtis distance matrix to explain the difference of sample groups based on the R package 'vegan'. The Canonical Correspondence Analysis (De Agostini et al.) was also performed by R package 'vegan' to analyze the relationships between geochemical parameters and the microbial community in different groups. The Random Forest (Numberger, #24) prediction was conducted in R using the 'randomForest' package. The comparison between different groups was determined using one-way analysis of variance (Dell'Anno et al.) and SPSS software (v8.0) and was considered significant at $P < 0.05$. All the statistical tests were performed using R 4.1.0 unless otherwise stated.

3. Results

3.1 Geochemical characteristics of soil

The geochemical parameters, including selected soil properties and heavy metal(loid) concentrations of 18 soil samples (from Y, XY, YBS, and ZD sites) are summarized in Fig. 2 and Fig. S1. The pH values of soil samples ranged from pH 3.88 to pH 8.37 and were not significantly different (ANOVA, $P > 0.05$) among the four sites. The oxidation-reduction potential (ORP) was significantly higher (ANOVA, $P < 0.05$) in Y and YBS sites than in XY and ZD sites. The total nitrogen content in the Y site was significantly higher (ANOVA, $P < 0.05$) compared to the other sites. In addition, the total organic carbon (TOC) concentration in the XY site was significantly lower ($P < 0.05$) than those in the Y and ZD sites. No significant differences in moisture content (MC) or sulfate concentrations were observed among the four sites.

The total concentrations of 14 heavy metal(loid)s, including Al, As, Cd, Cr, Cu, Fe, Mg, Mn, Ni, Pb, Sb, Ti, V, and Zn were determined (Fig. 2). Specifically, the Cd, Cr, Fe, Mn, Ti, V, and Zn concentrations in Y samples were significantly higher (ANOVA, $P < 0.05$) than those in XY and ZD sites. There were no significant differences in concentrations of Al, As, Cu, Mg, Ni, Pb, and Sb among the four sites. It is worth noting that the total concentrations of As, Cr, and Sb in all samples greatly exceeded the background limits of the Chinese soil standard (CSL, GB15618-2018), confirming that the Huilong plant (XY, YBS, and ZD sites) and its nearby areas (Y site) were highly polluted by various heavy metal(loid)s; especially As, Cr, and Sb being the main pollutants. BCR sequential extraction showed that the bioavailable fraction of metal(loid)s in the ZD site was higher than those in the other three sites, except for

249 the As and Cd species (Fig. S2).

250 *3.2 Diversity and taxonomic characteristics of microbial communities*

251 The sequences of 16S rRNA and ITS1 genes were amplified by Illumina Miseq
252 sequencing to analyze the bacterial and fungal compositions. After quality filtration, chimeras
253 were removed and sequences were assembled, a total of 1,211,767 high-quality reads were
254 obtained from the 18 samples for bacteria, and 1,003,712 high-quality reads were obtained
255 from the 17 samples for fungi (sample YBS5 did not successfully amplify fungi, maybe
256 because the fungal biomass was too low). The bacterial reads ranged from 37,345 to 74,602,
257 whereas the reads of fungi ranged from 39,272 to 74,314. Based on the 97% sequence
258 similarity, a total of 9,704 and 2,638 OTUs were identified with valid reads for the bacterial
259 and fungal communities, respectively. All coverage indices were > 0.98, indicating that the
260 reads libraries were reliable for the subsequent study and that the sequences typified the
261 actual bacterial and fungal communities (Fig. S3). For the bacterial community, the Chao
262 index was 2301.93 ± 897.79 (mean ± SD) (ranging from 3195.94 to 225.60), the Simpson
263 index was 0.02 ± 0.02 (from 0.005 to 0.084) and the Shannon index was 5.32 ± 0.92 (from
264 6.31 to 3.50). Although slight biases were observed in these indices, there were no significant
265 differences (ANOVA, $P > 0.05$) in bacterial community diversity and richness between these
266 four sites. Fungal community diversity showed that the Chao index (ranging from 1061.85 to
267 35.50) and Shannon index (from 4.74 to 1.81) in the XY site were significantly higher than
268 those in the Y site (ANOVA, $P < 0.05$). No significant differences in the Simpson index
269 (ranging from 0.35 to 0.03) were observed among the four sites (ANOVA, $P > 0.05$). These
270 results indicated that the alpha diversity of bacterial communities in different regions was not

significantly different, whereas a slight difference was observed in fungal communities.

PCoA analysis was calculated based on the sequences to determine the differences in the microbial communities among different sites (Fig. S4). PCoA1 and PCoA2 explained 15.81% and 13.22% of the variation of the bacterial community, respectively. Similarly, PCoA1 and PCoA2 explained 13.06% and 9.36% of the variation of fungal community, respectively. It was worth noting that the Y samples clustered separately, compared to the other three site samples (XY, YBS, and ZD sites) that were closely clustered. These results demonstrated that microbial communities were clustered by their corresponding origin. Taxonomic assignment analysis showed that a total of 65 bacterial and 14 fungal phyla were identified in the OTUs dataset. Among these, 14 bacterial phyla comprised > 90% of the whole raw reads (Fig. S6A), which included four bacterial dominant phyla (the relative abundance > 5%) of *Pseudomonadota* (24.43%-48.84%), *Chloroflexi* (8.92%-19.94%), *Actinobacteriota* (7.05%-15.74%), and *Acidobacteriota* (5.96%-10.38%). The dominant phyla *Pseudomonadota* were composed of *Alphaproteobacteria* and *Gammaproteobacteria* classes, which contributed to 20.57% and 21.48% of the bacterial community, respectively. And the dominant phyla *Actinobacteriota* in the Y site had higher relative abundances than the ZD site ($P < 0.05$) (Fig. S7A). Also, the relative abundances of some bacteria (such as the *Bacillota* phylum) in the YBS site were significantly higher ($P < 0.05$) than those at the XY and ZD sites (Fig. S7A). In addition, other phyla with low relative abundances were also identified among samples (Fig. S7A), such as *Bacteroidota*, *Desulfobacterota*, *Bacillota*, *Gemmatimonadota*, *Methylomirabilota*, *Patescibacteria*, *Planctomycetota*, etc.

For the fungal community, *Ascomycota* (21.40%-57.32%) and *Basidiomycota*

(3.42%-17.13%) were the dominant fungal phyla among four sites (except for the Y site) (Fig. S6B). The dominant phylum *Ascomycota* was significantly lower in the Y site than in the other three sites ($P < 0.05$). Also, the relative abundance of fungi-like *Basidiomycota* phylum in the Y site was significantly lower ($P < 0.05$) than that in the ZD site. In contrast, the relative abundances of some fungi (such as *Monoblepharomycota* and *unclassified_k__Fungi* phyla) in the Y site were significantly higher ($P < 0.05$) than those at the YBS and ZD sites (Fig. S7B). Additionally, the phyla *unclassified_k__Fungi* accounted for the fungal sequences with a relative abundance of 59.66% in the Y site, 32.38% in the XY site, 14.74% in the YBS site, and 18.92% in the ZD site, indicating that many unknown species existed in the fungal community. The above results indicated that there were significant differences in the distribution of bacterial and fungal communities in different smelting areas.

3.3 The importance of geochemical properties on microbial communities

RDA (Redundancy analysis) analysis (Fig. S4 and Fig. S5) and the RF (Random Forest) model (Fig. 3 and Fig. S8) were used to determine the role of geochemical properties on bacterial and fungal communities, respectively. According to the RDA analysis, the geochemical variables (RDA1 39.5%, RDA2 25.12% for the edaphic variables; RDA1 24.34%, RDA2 17.04% for the total metal(loid)s; RDA1 25.5%, RDA2 20.16% for the bioavailable metal(loid)s) explained the variations of bacterial communities (Fig. S4c,e and Fig. S5A), whereas the geochemical variables (RDA1 40.83%, RDA2 19.89% for the edaphic variables; RDA1 26.49%, RDA2 11.49% for the total metal(loid)s; RDA1 24.23%, RDA2 18.03% for the bioavailable metal(loid)s) explained the variations of the fungal communities (Fig. S4d,f and Fig. S5B). The relative abundance of the geochemical variables that affected

315 the beta diversity (NMDS1) was also predicted by the RF model (Fig. 3 and Fig. S8), which
316 explained 50.69% and 31.74% of the total variations of bacterial and fungal communities,
317 respectively. For bacteria, the Fe_bio and the TOC were the most important geochemical
318 variables on the beta diversity, which explained more than 15% of the variations, followed by
319 Cr_bio, Al_bio, Ni_bio, Zn_bio, and other environmental factors (Fig. 3). Many bioavailable
320 metal(loid)s showed positive effects on the beta diversity, such as Fe_bio, Ni_bio, Zn_bio,
321 V_bio, Mn_bio, As_bio, Sb_bio, and Ti_bio, whereas edaphic properties such as TN showed
322 negative impacts on the beta diversity of bacterial communities. The effects of other
323 geochemical variables on beta diversity were not clear and will not be further discussed. For
324 fungi, the dominant environmental factors were TN and As_bio, which explained more than
325 10% of the variations. Sulfate, as well as the Pb_bio, Cu_bio, and Cr_bio also influenced the
326 beta diversity of fungal communities (the relative abundance was more than 2%). The As_bio,
327 Ni_bio, and Pb_bio were positively related to the beta diversity, whereas the TN and Cd_bio
328 were negatively related to the beta diversity (Fig. S8).
329 The interactions between geochemical variables and microbial taxa (the top 500
330 abundant OTUs of bacterial (Table S1) and fungal (Table S2) communities) were further
331 analyzed using co-occurrence networks, with Spearman's correlations ($|R| > 0.6$ and $P < 0.05$)
332 (Fig. 4). For the bacterial community, Fe_bio had the most important impact on 25 OTUs,
333 which agreed well with the results of the Random Forest model. Cr_bio also had important
334 impacts on the bacterial community (13 OTUs), followed by Ni_bio (12 OTUs), the moisture
335 content (MC) (12 OTUs), and Fe_tot (10 OTUs) (Fig. 4A). A total of 88 OTUs displayed
336 significant correlations with geochemical variables, and the network was divided into ten

modules. The microbial taxa of *Burkholderiaceae* (2 OTUs), *Chitinophagaceae* (2 OTUs), *Comamonadaceae* (4 OTUs), *Hyphomonadaceae* (1 OTUs), *Nocardiaceae* (3 OTUs), *norank_o__IMCC26256* (1 OTUs), *norank_o__norank_c__P2-11E* (1 OTUs), *Oxalobacteraceae* (2 OTUs), *Rhodocyclaceae* (3 OTUs), *UBA12409* (1 OTUs), and *unclassified_c__Acidimicrobiia* (1 OTUs) families displayed the highest correlations with geochemical variables (Table S2). Some groups, such as *Chitinophagaceae*, *Comamonadaceae*, *Nocardiaceae*, *Oxalobacteraceae*, *Rhodocyclaceae,* and *UBA12409*, showed positive correlations with the bioavailable fractions of metals (Table S3). For the fungal community, a total of 135 OTUs displayed strong correlations with the geochemical variables, and the network was divided into eight modules. Mn_tot had the most important impact on 85 OTUs, followed by Cr_tot (79 OTUs), Ni_tot (62 OTUs), TOC (57 OTUs), V_tot (43 OTUs), and MC (30 OTUs) (Fig. 4B). The OTUs affiliated with the *Didymosphaeriaceae* (5 OTUs), *Fomitopsidaceae* (3 OTUs), *Lophiostomataceae* (2 OTUs), *Lycoperdaceae* (3 OTUs), *Meruliaceae* (12 OTUs), *Phaeosphaeriaceae* (5 OTUs), *Pleosporaceae* (4 OTUs), *Steccherinaceae* (3 OTUs), and *Xenasmataceae* (2 OTUs) families were strongly influenced by multiple environmental parameters. These families (except for *Lophiostomataceae* and *Xenasmataceae*) showed positive correlations with the bioavailable fractions of metal(loid)s, whereas negative correlations were found with the total metal(loid) content and the other environmental parameters (Table S4).

3.4 Co-occurrence patterns and keystone taxa analysis of microbial communities

In the present study, the co-occurrence patterns of bacterial and fungal communities were individually constructed by strong correlations (Spearman $R > |0.6|$) and significant ($P <$

0.05) among the top 500 abundant OTUs in the Huilong smelter regions. For bacteria, the networks of the Huilong smelter regions contained 473 nodes (OTUs) and 5120 edges (connection between OTUs). Whereas for fungi, the networks of the Huilong smelter regions contained 490 nodes and 16559 edges. Analogously, the average degree, clustering coefficient, and density in fungal communities were higher than those in bacterial communities. It was worth noting that, the proportions of positive edges tended to be higher than negative edges in the networks of bacterial and fungal communities (Table 1). Moreover, the nodes were assigned by phylum (Fig. 5A and C) and modularity class (Fig. 5B and D).

A total of 11 dominant taxa (at the phylum level) were identified from the co-occurrence patterns of bacterial communities, which accounted for 86.26% of total nodes, and the remaining modes (65 nodes) were classified as others (13.74%). *Pseudomonadota* was the most dominant phylum, which accounted for 32.98% of total nodes, followed by *Actinobacteriota* (10.99%), *Chloroflexi* (7.82%), *Acidobacteriota* (5.92%), *Planctomycetota* (5.5%), and *Bacteroidota* (5.5%) in the bacterial networks (Fig. 5A). All nodes were divided into 11 modules, including 5 major modules (Fig. 5B). Additionally, the OTUs with nodes degree > 30 and betweenness centrality < 100 were typically identified as the keystone phylotypes in the present study. Here a total of 5 nodes were identified as the keystone taxa, which are mainly distributed in Module III and Module IV. The keystone OTUs were affiliated to *Diplorickettsiaceae*, *norank_o__Candidatus_Woesebacteria*, *norank_o__norank_c__AT-s3-28*, *norank_o__norank_c__bacteriap25*, and *Phycisphaeraceae* families.

Accordingly, for fungi, a total of 11 phyla (Fig. 5C), including *Ascomycota* (51.84%),

Basidiomycota (41.63%), *Glomeromycota* (2.24%), *Chytridiomycota* (2.04%), *Rozellomycota* (0.61%), *Mucoromycota* (0.41%), *Olpidiomycota* (0.41%), *Mortierellomycota* (0.2%), *Kickxellomycota* (0.2%), *Calcarisporiellomycota* (0.2%) and *Monoblepharomycota* (0.2%), were identified from the co-occurrence patterns of fungal communities. All nodes were divided into 9 modules, including 6 major modules (Fig. 5D). Here a total of 9 nodes were identified as the keystone OTUs, which were affiliated to *Biatriosporaceae*, *Ganodermataceae*, *Peniophoraceae*, *Phaeosphaeriaceae*, *Polyporaceae*, *Teichosporaceae*, *Trichomeriaceae*, *Wrightoporiaceae*, *Xylariaceae* families, mainly distributing in Module I, Module III and Module IV.

3.5 Ecological assembly processes of microbial communities

The calculated βNTI and RC_{bray} were compared between bacterial and fungal communities, and the assembly processes were determined. There were slight differences in the scale of the assembly process at each site. The assembly process was judged according to the criteria described in the above method. For the whole bacterial communities, the majority of the βNTI in the whole microbial community (91.5%) was greater than 2, indicating that the deterministic process controlled the bacterial community assembly (Fig. 6A). The Y and YBS sites had similar assembly processes, with the variable selection accounting for 94.5% and undominated process accounting for 5.5%. Similarly, the variable selection process (90.1% and 87.7%) also governed the bacterial community assembly of XY and ZD sites, whereas the dispersal limitation (4.4% and 2.3%) and undominated (5.5% and 10%) incurred variations in bacterial communities of the XY and ZD sites, respectively. For the whole fungal communities, the relative contribution of the deterministic process (90.2%) was higher

than that of the stochastic process (9.8%) (Fig. 6B). Within fungal communities of each site, variable selection accounted for a high percentage of community assembly, including Y (82.3%), XY (92.9%), YBS (91.2%), and ZD sites (90.5%). The stochastic process contained dispersal limitation (7.9%), homogenizing dispersal (3.9%), and undominated (5.9%) in the Y site, whereas only undominated processes (7.1%, 8.8%, and 9.5%) were present in the XY, YBS, and ZD sites, respectively. These results indicated that deterministic processes dominated the assembly of microbial communities regardless of bacterial or fungal communities.

A correlation matrix between edaphic variables and the βNTI was assembled to investigate the factors influencing the ecological assembly process of microbial communities. The assembly process of bacterial communities was more affected by the tested geochemical properties than the fungal communities (Table S1). In particular, the pH, TN, total metal(loid)s, and the bioavailable fractions of metal(loid)s (except for As, Cd, and Ti) had significant impacts on either the bacterial or fungal assembly processes in this study (Table S1-1).

4. Discussion

Metal(loid)s pollution of soil is a high-priority research topic in which microbial strategies for stabilizing metal(loid)s are recognized as a promising alternative relative to traditional remediation technologies. Microbial communities are identified as potential indicators of soil function and health in contaminated and surrounding environments (Banerjee and van der Heijden, 2022). Most recent studies of metal(loid)s contamination focus on only one microbial domain at a time (Park et al., 2021; Liu et al., 2022a; Liu et al.,

2022c; Zhang et al., 2022c). However, the co-occurrence patterns and ecological assembly processes of both bacterial and fungal communities under diverse metal(loid)s exposures have not been investigated so far. Therefore, it is necessary to comprehensively compare the responses of indigenous bacterial and fungal communities to metal(loid)s pollution.

4.1 Geochemical characterizations

In the Huilong smelter area, the concentrations of total As, Cr, and Sb exceeded the Chinese *Soil Environmental Quality Construction Land Soil Pollution Risk Management and Control Standard (Trial)* (GB36600-2018), which is the second land use standard for screening purposes. Although no significant differences in these total metal(loid)s concentrations (except for total Cr) were found among the four studied sites. In contrast, significant differences were observed in the bioavailable fraction of these metal(loid)s among the four contaminated areas. For example, the bioavailable fraction proportion of As (As_bio) in three sites (XY, YBS, and ZD) was higher than that in the Y site (Fig. S2). Recent studies of the evaluation of metal(loid)s pollution risk at other sites of the Huilong smelter (Li et al., 2022a) showed that the high-risk metal elements were As and Sb. These results suggested that smelting activities released these metal(loid)s to the local community, despite being shut down more than two decades ago. Additionally, both TN and TOC were significantly higher in the Y site than in the other three sites. It was likely that the Y site was located near farmland, as the levels of TN and TOC in agricultural soils tend to be higher than in other soil types (Compton et al., 2004). Therefore, the above results indicated that significant differences were observed in metal(loid)s and environmental factors between the Huilong smelter area (XY, YBS, and ZD sites) and the surrounding area (Y site), which might be

related to the artificial smelting activities.

4.2 Effects of geochemical characteristics on bacterial and fungal communities

There were no significant differences in bacterial diversity and richness (Fig. S3A). Such observations demonstrate that the alpha diversity of bacterial communities was not significantly affected by the variations of metal(loid)s and environmental factors, which is similar to previous studies of metal(loid)s contaminated environments near mining and smelting sites (Pereira et al., 2014; Chun et al., 2021; Liu et al., 2021). In contrast, significant differences in alpha diversity (except the Simpson indices) and richness were observed for fungi. From the perspective of microbial diversity, the toxic effects of metal(loid)s can often reduce microbial diversity during the initial phase of metal(loid)s exposure (Liu et al., 2022a). However, the microbes could then develop an adaptive response mechanism to metal(loid)s contamination, as evidenced by an increase in their diversity and richness (Yan et al., 2020). In particular, the diversity and richness of fungal communities in the XY site (in Huilong smelter area) were significantly higher than in the Y site (in the surrounding area), which demonstrated that smelting activities maybe increase the fungal diversity and richness.

Notably, beta-diversity patterns were distinguished in both bacterial and fungal communities, with significant differences among the four sites as revealed by PCoA (Fig. S4) and RDA analyses (Fig. S4 and S5). Such observations may be due to the combined effect of metal(loid)s and other geochemical parameters. The RF model prediction showed that the bioavailability of certain metal(loid)s (Al, As, Cr, Fe, Ni, Pb, Sb, Ti, and Zn) had positive effects on the beta-diversity of bacterial communities (Fig. 3). Similarly, bioavailable As, Ni, and Pb had positive effects on the beta diversity of fungal communities (Fig. S8). These

results suggest that the bioavailable fractions of metal(loid)s have substantial impacts on the beta diversities of the bacterial and fungal communities (Wang et al., 2018), although the dominant factors differed for the bacterial and fungal communities. As previously reported, bioavailable Al, As, Fe, and Sb have strong negative effects on microbial diversity (Liu et al., 2022c) and significant decreases in community richness in As-and Cr-contaminated soils (Sheik et al., 2012). In contrast, the bioavailable fractions of certain metal(loid)s presented here generally showed positive effects on the beta diversity of microbial communities, as shown in the RF model, probably due to sensitive indigenous microorganisms that were stimulated by the metal(loid)s.

The microbial-contaminant interactions demonstrated that some bacteria and fungi were responsive to some but not all bioavailable metals in soil. For example, three OTUs associated with *Comamonadaceae* showed positive relationships with the bioavailable Fe, Cr, and Ni. Members of *Comamonadaceae* have been identified as Fe(III)-reducing bacteria, which could adapt to the detrimental environment by changing their metabolic ways (Wang et al., 2021; Zhang et al., 2022a). Consistently, two OTUs associated with *Rhodocyclaceae* showed positive relationships with the bioavailable Fe and Cr. It also has been reported that Pb exhibited a strong correlation with the Fe(III)-reducing bacterial lineages *Rhodocyclaceae* (Moberly et al., 2016; Jia et al., 2022). Apart from these bacteria, the fungi, e.g., *Meruliaceae* and *Pleosporaceae,* showed similar trends. Members of *Meruliaceae* were the most influenced by multiple environmental parameters, three OTUs associated with *Meruliaceae* showed positive relationships with the bioavailable Fe, Ni, and V. Although *Meruliaceae* often grows on rotten gymnosperm wood (Liu et al., 2022e), the relationship of *Meruliaceae*

with metal(loid)s has not been studied. Additionally, two OTUs associated with *Pleosporaceae* showed positive relationships with the bioavailable Fe and V. It was consistent with the observation of rhizosphere fungal communities in a Cu tailings area (Jia et al., 2020). The observations presented here demonstrate the adaptation of the promising candidates (e.g., bacteria, *Comamonadaceae*, *Rhodocyclaceae*, and fungi, *Meruliaceae*, *Pleosporaceae*) to the conditions prevailing at Huilong nonferrous metal smelter.

4.3 The co-occurrence patterns of bacterial and fungal communities

Soil microbes do not thrive well in isolated environments; instead, they prefer complex networks of interactions. In the present study, the co-occurrence patterns of bacterial and fungal communities were established using networks based on the random matrix theory to reveal the interactions between microbes (Faust and Raes, 2012). The topological characteristics of networks generally represent the levels of interactions and connectedness (Zheng et al., 2018). Compared to bacterial networks, the fungal networks had more links (Table 1 and Fig. 5), which indicated that inter-species relationships among different adaptive fungal species would be strengthened and stabilized in metal(loid)s contaminated areas. On the other hand, the bacterial communities were less adapted and were weaker as evidenced by their few inter-species relationships. These data suggest that fungal communities were less sensitive and more resistant to HM toxicity than the bacterial communities residing at this abandoned smelter site. These results indicated that the frequency of connections for fungal communities was higher than those in bacterial communities. Generally, there were similar trends in network topological properties for both bacterial and fungal communities.

The keystone species inhabiting the heavily polluted areas may indicate that they have

special ecological roles in harsh environments. In the present study, the OTU with nodes degree > 30 and betweenness centrality < 100 were typically identified as the keystone phylotypes. In the bacterial networks, the members of the family *Diplorickettsiaceae*, *norank_o__Candidatus_Woesebacteria*, *norank_o__norank_c__AT-s3-28*, *norank_o__norank_c__bacteriap25*, and *Phycisphaeraceae* were considered as the keystone taxa in the bacterial communities. Within these keystone taxa, members of *Diplorickettsiaceae*, belonging to the phylum of *Pseudomonadota*, have been identified as Pb-sensitive taxa in the soil microbial community (Wan et al., 2022). Consistently, several previous studies have shown that the members of *Pseudomonadota* possess a large number of metal-related operons, which are responsible for the detoxification of metal(loid)s (Qiao et al., 2021; Zou et al., 2021). The *Pseudomonadota* was abundant in the Huilong area, suggesting that this phylum mitigates metal(loid)s toxicity through a special adaptive mechanism (Keshri et al., 2015; Fashola et al., 2016). Moreover, members of *norank_o__Candidatus_Woesebacteria* belong to the phylum of *Patescibacteria*, which phyla has As, Fe, and Ag resistance genes (Zhou et al., 2022) and can transport various heavy metals from massive soils to the rhizosphere (Tian et al., 2022). Consistent with previous studies (Flieder et al., 2020; Liu et al., 2022c), the members of *norank_o__norank_c__AT-s3-28* family, associated with the phylum *Acidobacteriota*, play a key role in bacterial communities in areas such as Huilong, which exhibited a resistance capacity to metal(loid)s pollution (Wang et al., 2022a). It is not surprising that the family *norank_o__norank_c__bacteriap25* (*Myxococcota*) and *Phycisphaeraceae* (*Planctomycetota*) were identified as keystone taxa in the Huilong site, owing to their ability to tolerate and

resist metals ions using the complexation and adsorption mechanisms (Dell'Anno et al., 2021; Liu et al., 2022d; Marghoob et al., 2022; Gao et al., 2022). These findings could help develop remediation strategies for Huilong contaminated areas, for example, by purposefully screening key species for biological materials.

The fungi with a strong resistance to metal(loid)s pollution can play a key role in the restoration of metal(loid)s polluted ecosystems. In the fungal networks, OTUs affiliated to the *Biatriosporaceae (Ascomycota)*, *Ganodermataceae (Basidiomycota)*, *Peniophoraceae (Basidiomycota)*, *Phaeosphaeriaceae (Ascomycota)*, *Polyporaceae (Basidiomycota)*, *Teichosporaceae (Ascomycota)*, *Trichomeriaceae (Ascomycota)*, *Wrightoporiaceae (Basidiomycota)*, *Xylariaceae (Ascomycota)* families were considered as the keystone taxa. These OTUs mainly belonged to the phylum of *Ascomycota* and *Basidiomycota*. *Ascomycota*, the most abundant and widely existing soil fungi in the world, was the keystone phylum in the fungal networks of Huilong sites, consistent with the previous studies (Lin et al., 2019; De Agostini et al., 2020; Xie et al., 2021). This phylum has a strong tolerance to metal(loid)s; in fact, even its abundance was increased with metal(loid)s concentrations (Lin et al., 2019). Furthermore, *Basidiomycota* was also a dominant phylum in the networks of fungal communities. *Basidiomycota* (filamentous fungi) can be used to remove metal(loid)s (Chen et al., 2012). Therefore, *Basidiomycetes* could be associated with their adaptation and function in metal(loid)s contaminated environments. These results agree with a previous report (Chen et al., 2014) that *Ascomycota* and *Basidiomycota* were the most important components in metal(loid)s polluted soils.

In addition, positive and negative links (representing positive and negative correlations)

may reflect cooperation (or niche overlap) and competition (or niche separation) among species (Deng et al., 2016; Ghoul and Mitri, 2016; Zhang et al., 2018). Here there were more positive links than negative links in both bacterial and fungal networks (Table 1). This reflects the importance of microbial synergy, where most microbial species potentially cooperate to withstand metal(loid)s pollution (Hoek et al., 2016). It is worth noting that the proportion of positive connections is significantly higher in fungal networks than in bacterial networks. This indicates that environmental pollution at the studied Huilong factories, as well as other anthropogenic sources, increased the competition of species among the fungal community (Zhou et al., 2020). Competition can stabilize the co-oscillation of the community and promote the stability of the network (Coyte et al., 2015).

4.4 Ecological assembly processes of bacterial and fungal communities

Revealing the assembly process of the microbial community in ecological niches can uncover the responses of a microbial community to perturbations by metal(loid) exposures (Jiao et al., 2016; Zhang et al., 2021; Liu et al., 2022a). In the current study, variable selection accounted for the highest contribution rate (82.3-94.5%) in the deterministic process among bacterial and fungal communities (Fig. 6). However, the stochastic processes contribute differently to the assemblies of fungal and bacterial communities. For example, the fungal community showed a stronger dispersal limitation than the bacterial community in the influenced area (Y site), which was consistent with previous studies (Jiang et al., 2016). That it is because the body size of fungi hindered their spread or spatial aggregation, and limited long distance dispersal compared with the smaller bacteria (Xu et al., 2021b). An opposite trend occurred in Huilong factories area (XY, YBS, and ZD sites), in which high levels of

dispersal limitation were found in bacterial communities, possibly due to the differences of metal(loid) consentrations and geochemical properties between the influenced area (Y site) and Huilong factories area (XY, YBS, and ZD sites). Above observations agreed with several previous studies (Zhou and Ning, 2017; Mori et al., 2018; Zheng et al., 2021) reporting that the deterministic and stochastic processes could jointly regulate the natural community assembly, and their relative importance varies with the environmental context. Furthermore, the present study showed that the pH, TN, total metal(loid) concentrations, and the bioavailable fractions of metal(loid)s (except for the As, Cd, and Ti) had significant impacts on the microbial assembly process. These results confirm the combined effect of metal(loid) exposures and geochemical properties on the microbial community. However, ecological deterministic and stochastic processes exist that can jointly contribute to the soil microbial community assembly in response to metal(loid)s exposure. Their detailed contributions can vary in bacterial and fungal communities depending on the environmental context.

5. Conclusion

The response of bacterial and fungal communities to different geochemical variables, as well as their ecological assembly processes, were investigated in the present study. The smelting activities had indeed brought metal(loid)s pollution, especially As and Sb, to the locality, although Huilong smelter has been shut down for decades. Both metal(loid)s and edaphic variables drive the microbial communities, but very different responses of innate microbiota were observed. The bioavailable Fe and TOC had considerable impacts on the beta diversity of bacterial communities, whereas TN and bioavailable As mainly influenced the fungal communities. The inter-species interactions of fungal co-occurrence networks were

more complex than the bacterial networks, suggesting inter-species relationships among different fungal species were more stable than the bacterial species in this metal(loid)s contaminated area. Moreover, the relatively higher positive interaction of microbiota indicated the importance of microbial synergy among species with stronger resistance to metal(loid)s polluted environments. The keystone taxa were investigated and revealed their adaptive superiority to metal(loid)s stress. Additionally, the deterministic process (variable selection) dominated all bacterial and fungal assemblies, which was highly impacted by the pH, TN, total metal(loid)s, and the bioavailable fractions of certain metal(loid)s. These findings enhance our understanding of the microbial responses to anthropogenically induced smelting activities and provide a vital guideline for developing the bioremediation practice of metal(loid)s contaminated sites.

Acknowledgments

This work has been supported partly by grants received from the Major National R & D Projects from the Chinese Ministry of Science and Technology (2019YFC1803500), the National Science Foundation of China (42230716, 41720104007), the 111 Project (B21017), and the 1000-Talents Plan project (WQ2017110423).

Author contributions

Miaomiao Li: Conceptualization, Methodology, Resources, Formal analysis, Writing - original draft, Writing – review & editing. **Jun Yao:** Writing – review & editing, Funding acquisition. **Geoffrey Sunahara, Robert Duran** and **Qinghua Zhang:** Conceptualization, Data Curation, Visualization, Writing – review & editing. **Bang Liu**, **Ying Cao**, **Hao Li,**

Wancheng Pang, **Houquan Liu, Shun Jiang, Junjie Zhu:** Writing – review & editing.

Conflicts of interest

The authors declare that there are no conflicts of interest.

References

Aponte, H., Herrera, W., Cameron, C., Black, H., Meier, S., Paolini, J., Tapia, Y., Cornejo, P., 2020. Alteration of enzyme activities and functional diversity of a soil contaminated with copper and arsenic. Ecotoxicol Environ Saf. 192, 110264. 10.1016/j.ecoenv.2020.110264

Banerjee, S., van der Heijden, M.G.A., 2022. Soil microbiomes and one health. Nat Rev Microbiol. 10.1038/s41579-022-00779-w

Barberan, A., Bates, S.T., Casamayor, E.O., Fierer, N., 2012. Using network analysis to explore co-occurrence patterns in soil microbial communities. ISME J. 6(2), 343-51. 10.1038/ismej.2011.119

Chen, G., Fan, J., Liu, R., Zeng, G., Chen, A., Zou, Z., 2012. Removal of Cd(II), Cu(II) and Zn(II) from aqueous solutions by live Phanerochaete chrysosporium. Environ Technol. 33(22-24), 2653-9. 10.1080/09593330.2012.673015

Chen, J., He, F., Zhang, X., Sun, X., Zheng, J., Zheng, J., 2014. Heavy metal pollution decreases microbial abundance, diversity and activity within particle-size fractions of a paddy soil. FEMS Microbiol Ecol. 87(1), 164-81. 10.1111/1574-6941.12212

Chun, S.J., Kim, Y.J., Cui, Y., Nam, K.H., 2021. Ecological network analysis reveals distinctive microbial modules associated with heavy metal contamination of abandoned mine soils in Korea. Environ Pollut. 289, 117851. 10.1016/j.envpol.2021.117851

Compton, J.E., Watrud, L.S., Arlene Porteous, L., DeGrood, S., 2004. Response of soil microbial biomass and community composition to chronic nitrogen additions at Harvard forest. Forest Ecology and Management. 196(1), 143-158. 10.1016/j.foreco.2004.03.017

650 Coyte, K.Z., Schluter, J., Foster, K.R., 2015. The ecology of the microbiome: networks,
651 competition, and stability. Science. 350, 663-666.
652 De Agostini, A., Caltagirone, C., Caredda, A., Cicatelli, A., Cogoni, A., Farci, D., Guarino, F.,
653 Garau, A., Labra, M., Lussu, M., Piano, D., Sanna, C., Tommasi, N., Vacca, A., Cortis,
654 P., 2020. Heavy metal tolerance of orchid populations growing on abandoned mine
655 tailings: A case study in Sardinia Island (Italy). Ecotoxicol Environ Saf. 189, 110018.
656 10.1016/j.ecoenv.2019.110018
657 Dell'Anno, A., Beolchini, F., Rocchetti, L., Luna, G.M., Danovaro, R., 2012. High bacterial
658 biodiversity increases degradation performance of hydrocarbons during
659 bioremediation of contaminated harbor marine sediments. Environmental Pollution.
660 167, 85-92. 10.1016/j.envpol.2012.03.043
661 Dell'Anno, F., Rastelli, E., Tangherlini, M., Corinaldesi, C., Sansone, C., Brunet, C., Balzano,
662 S., Ianora, A., Musco, L., Montereali, M.R., Dell'Anno, A., 2021. Highly
663 Contaminated Marine Sediments Can Host Rare Bacterial Taxa Potentially Useful for
664 Bioremediation. Front Microbiol. 12, 584850. 10.3389/fmicb.2021.584850
665 Deng, Y., Zhang, P., Qin, Y., Tu, Q., Yang, Y., He, Z., Schadt, C.W., Zhou, J., 2016. Network
666 succession reveals the importance of competition in response to emulsified vegetable
667 oil amendment for uranium bioremediation. Environ Microbiol. 18(1), 205-18.
668 10.1111/1462-2920.12981
669 Dettmann, U., Kraft, N.N., Rech, R., Heidkamp, A., Tiemeyer, B., 2021. Analysis of peat soil
670 organic carbon, total nitrogen, soil water content and basal respiration: Is there a ‘best’
671 drying temperature? Geoderma. 403. 10.1016/j.geoderma.2021.115231
672 Fashola, M.O., Ngole-Jeme, V.M., Babalola, O.O., 2016. Heavy Metal Pollution from Gold
673 Mines: Environmental Effects and Bacterial Strategies for Resistance. Int J Environ
674 Res Public Health. 13(11). 10.3390/ijerph13111047
675 Faust, K., Raes, J., 2012. Microbial interactions: from networks to models. Nat Rev
676 Microbiol. 10(8), 538-50. 10.1038/nrmicro2832
677 Fei, X., Christakos, G., Xiao, R., Ren, Z., Liu, Y., Lv, X., 2019. Improved heavy metal
678 mapping and pollution source apportionment in Shanghai City soils using auxiliary
679 information. Sci Total Environ. 661, 168-177. 10.1016/j.scitotenv.2019.01.149

Feng, M., Adams, J.M., Fan, K., Shi, Y., Sun, R., Wang, D., Guo, X., Chu, H., 2018. Long-term fertilization influences community assembly processes of soil diazotrophs. Soil Biology and Biochemistry. 126, 151-158. 10.1016/j.soilbio.2018.08.021

Flieder, M., Buongiorno, J., Herbold, C.W., Hausmann, B., Rattei, T., Lloyd, K.G., Loy, A., Wasmund, K., 2020. Novel taxa of Acidobacteriota involved in seafloor sulfur cycling. bioRxiv. 10.1101/2020.10.01.322446

Gao, W., Liu, P., Ye, Z., Zhou, J., Wang, X., Huang, X., Deng, X., Ma, L., 2022. Divergent prokaryotic microbial assembly, co-existence patterns and functions in surrounding river sediments of a Cu-polymetallic deposit in Tibet. Sci Total Environ. 851(Pt 1), 158192. 10.1016/j.scitotenv.2022.158192

Ghoul, M., Mitri, S., 2016. The Ecology and Evolution of Microbial Competition. Trends Microbiol. 24(10), 833-845. 10.1016/j.tim.2016.06.011

Hoek, T.A., Axelrod, K., Biancalani, T., Yurtsev, E.A., Liu, J., Gore, J., 2016. Resource Availability Modulates the Cooperative and Competitive Nature of a Microbial Cross-Feeding Mutualism. PLoS Biol. 14(8), e1002540. 10.1371/journal.pbio.1002540

Jia, S., Tian, Y., Li, J., Chu, X., Zheng, G., Liu, Y., Zhao, W., 2022. Field study on the characteristics of scales in damaged multi-material water supply pipelines: Insights into heavy metal and biological stability. J Hazard Mater. 424(Pt A), 127324. 10.1016/j.jhazmat.2021.127324

Jia, T., Guo, T.Y., Wang, R.H., Chai, B.F., 2020. Effects of heavy metal contents on phyllosphere and rhizosphere fungal communities for bothriochloa ischaemum in copper tailings area. Environmental Science. 41(11), 5193-5200.

Jiang, Y., Liang, Y., Li, C., Wang, F., Sui, Y., Suvannang, N., Zhou, J., Sun, B., 2016. Crop rotations alter bacterial and fungal diversity in paddy soils across East Asia. Soil Biology and Biochemistry. 95, 250-261. 10.1016/j.soilbio.2016.01.007

Jiao, S., Liu, Z., Lin, Y., Yang, J., Chen, W., Wei, G., 2016. Bacterial communities in oil contaminated soils: Biogeography and co-occurrence patterns. Soil. Biol. Biochem. 98, 64-73. 10.1016/j.soilbio.2016.04.005

Keshri, J., Mankazana, B.B., Momba, M.N., 2015. Profile of bacterial communities in South

African mine-water samples using Illumina next-generation sequencing platform. Appl Microbiol Biotechnol. 99(7), 3233-42. 10.1007/s00253-014-6213-6

Kim, E.J., Yoo, J.C., Baek, K., 2014. Arsenic speciation and bioaccessibility in arsenic-contaminated soils: sequential extraction and mineralogical investigation. Environ Pollut. 186, 29-35. 10.1016/j.envpol.2013.11.032

Li, H., Yao, J., Min, N., Chen, Z., Li, M., Pang, W., Liu, B., Cao, Y., Men, D., Duran, R., 2022a. Comprehensive evaluation of metal(loid)s pollution risk and microbial activity characteristics in non-ferrous metal smelting contaminated site. Journal of Cleaner Production. 344. 10.1016/j.jclepro.2022.130999

Li, M., Yao, J., Sunahara, G., Hawari, J., Duran, R., Liu, J., Liu, B., Cao, Y., Pang, W., Li, H., Li, Y., Ruan, Z., 2022b. Novel microbial consortia facilitate metalliferous immobilization in non-ferrous metal(loid)s contaminated smelter soil: Efficiency and mechanisms. Environ Pollut. 313, 120042. 10.1016/j.envpol.2022.120042

Lin, Y., Ye, Y., Hu, Y., Shi, H., 2019. The variation in microbial community structure under different heavy metal contamination levels in paddy soils. Ecotoxicol Environ Saf. 180, 557-564. 10.1016/j.ecoenv.2019.05.057

Liu, B., Yao, J., Chen, Z., Ma, B., Li, H., Wancheng, P., Liu, J., Wang, D., Duran, R., 2022a. Biogeography, assembly processes and species coexistence patterns of microbial communities in metalloids-laden soils around mining and smelting sites. J Hazard Mater. 425, 127945. 10.1016/j.jhazmat.2021.127945

Liu, B., Yao, J., Chen, Z., Ma, B., Liu, J., Li, H., Zhu, X., Li, M., Cao, Y., Pang, W., Zhao, C., Mihucz, V.G., Duran, R., 2022b. Unraveling ecological risk of As/Sb and other metal(loid)s and fungal community responses in As/Sb smelting-intensive zone: A typical case study of Southwest China. Journal of Cleaner Production. 338. 10.1016/j.jclepro.2022.130525

Liu, B., Yao, J., Ma, B., Chen, Z., Zhao, C., Zhu, X., Li, M., Cao, Y., Pang, W., Li, H., Feng, L., Mihucz, V.G., Duran, R., 2021. Microbial community profiles in soils adjacent to mining and smelting areas: Contrasting potentially toxic metals and co-occurrence patterns. Chemosphere. 282, 130992. 10.1016/j.chemosphere.2021.130992

Liu, B., Yao, J., Ma, B., Chen, Z., Zhu, X., Zhao, C., Li, M., Cao, Y., Pang, W., Li, H.,

Mihucz, V.G., Duran, R., 2022c. Metal(loid)s diffusion pathway triggers distinct microbiota responses in key regions of typical karst non-ferrous smelting assembly. J. Hazard. Mater. 423(Pt B), 127164. 10.1016/j.jhazmat.2021.127164

Liu, J., Bao, Z., Wang, C., Wei, J., Wei, Y., Chen, M., 2022d. Understanding of mercury and methylmercury transformation in sludge composting by metagenomic analysis. Water Res. 226, 119204. 10.1016/j.watres.2022.119204

Liu, Z.B., Zhang, J.L., Papp, V., Dai, Y.C., 2022e. Taxonomy and Phylogeny of Meruliaceae with Descriptions of Two New Species from China. J Fungi (Basel). 8(5). 10.3390/jof8050501

Magoc, T., Salzberg, S.L., 2011. FLASH: fast length adjustment of short reads to improve genome assemblies. Bioinformatics. 27(21), 2957-63. 10.1093/bioinformatics/btr507

Marghoob, M.U., Rodriguez-Sanchez, A., Imran, A., Mubeen, F., Hoagland, L., 2022. Diversity and functional traits of indigenous soil microbial flora associated with salinity and heavy metal concentrations in agricultural fields within the Indus Basin region, Pakistan. Front Microbiol. 13, 1020175. 10.3389/fmicb.2022.1020175

Moberly, J., D'Imperio, S., Parker, A., Peyton, B., 2016. Microbial community signature in Lake Coeur d'Alene: Association of environmental variables and toxic heavy metal phases. Applied Geochemistry. 66, 174-183. 10.1016/j.apgeochem.2015.12.013

Mori, A.S., Isbell, F., Seidl, R., 2018. beta-Diversity, Community Assembly, and Ecosystem Functioning. Trends Ecol Evol. 33(7), 549-564. 10.1016/j.tree.2018.04.012

Olesen, J.M., Bascompte, J., Dupont, Y.L., Jordano, P., 2007. The modularity of pollination networks. PNAS. 104 (50) 19891-19896.

Park, S.C., Boyanov, M.I., Kemner, K.M., O'Loughlin, E.J., Kwon, M.J., 2021. Distribution and speciation of Sb and toxic metal(loid)s near an antimony refinery and their effects on indigenous microorganisms. J Hazard Mater. 403, 123625. 10.1016/j.jhazmat.2020.123625

Pereira, L.B., Vicentini, R., Ottoboni, L.M., 2014. Changes in the bacterial community of soil from a neutral mine drainage channel. PLoS One. 9(5), e96605. 10.1371/journal.pone.0096605

Price, G.W., Langille, M.G.I., Yurgel, S.N., 2021. Microbial co-occurrence network analysis

of soils receiving short- and long-term applications of alkaline treated biosolids. Sci Total Environ. 751, 141687. 10.1016/j.scitotenv.2020.141687

Qiao, L., Liu, X., Zhang, S., Zhang, L., Li, X., Hu, X., Zhao, Q., Wang, Q., Yu, C., 2021. Distribution of the microbial community and antibiotic resistance genes in farmland surrounding gold tailings: A metagenomics approach. Sci Total Environ. 779, 146502. 10.1016/j.scitotenv.2021.146502

Sheik, C.S., Mitchell, T.W., Rizvi, F.Z., Rehman, Y., Faisal, M., Hasnain, S., McInerney, M.J., Krumholz, L.R., 2012. Exposure of soil microbial communities to chromium and arsenic alters their diversity and structure. PLoS One. 7(6), e40059. 10.1371/journal.pone.0040059

Sun, X., Kong, T., Xu, R., Li, B., Sun, W., 2020. Comparative characterization of microbial communities that inhabit arsenic-rich and antimony-rich contaminated sites: Responses to two different contamination conditions. Environ Pollut. 260, 114052. 10.1016/j.envpol.2020.114052

Tian, Z., Li, G., Tang, W., Zhu, Q., Li, X., Du, C., Li, C., Li, J., Zhao, C., Zhang, L., 2022. Role of Sedum alfredii and soil microbes in the remediation of ultra-high content heavy metals contaminated soil. Agriculture, Ecosystems & Environment. 339. 10.1016/j.agee.2022.108090

Wan, Y., Devereux, R., George, S.E., Chen, J., Gao, B., Noerpel, M., Scheckel, K., 2022. Interactive effects of biochar amendment and lead toxicity on soil microbial community. J Hazard Mater. 425, 127921. 10.1016/j.jhazmat.2021.127921

Wang, C., Jia, Y., Wang, Q., Yan, F., Wu, M., Li, X., Fang, W., Xu, F., Liu, H., Qiu, Z., 2022a. Responsive change of crop-specific soil bacterial community to cadmium in farmlands surrounding mine area of Southeast China. Environ Res. 214(Pt 1), 113748. 10.1016/j.envres.2022.113748

Wang, C., Liu, S., Wang, P., Chen, J., Wang, X., Yuan, Q., Ma, J., 2021. How sediment bacterial community shifts along the urban river located in mining city. Environ Sci Pollut Res Int. 28(31), 42300-42312. 10.1007/s11356-020-12031-0

Wang, N., Zhang, S., He, M., 2018. Bacterial community profile of contaminated soils in a typical antimony mining site. Environ Sci Pollut Res Int. 25(1), 141-152.

10.1007/s11356-016-8159-y

Wang, W., Wang, H., Cheng, X., Wu, M., Song, Y., Liu, X., Loni, P.C., Tuovinen, O.H., 2022b. Different responses of bacteria and fungi to environmental variables and corresponding community assembly in Sb-contaminated soil. Environmental Pollution. 298. 10.1016/j.envpol.2022.118812

Wei, G., Li, M., Shi, W., Tian, R., Chang, C., Wang, Z., Wang, N., Zhao, G., Gao, Z., 2020. Similar drivers but different effects lead to distinct ecological patterns of soil bacterial and archaeal communities. Soil Biology and Biochemistry. 144. 10.1016/j.soilbio.2020.107759

Xie, Y., Bu, H., Feng, Q., Wassie, M., Amee, M., Jiang, Y., Bi, Y., Hu, L., Chen, L., 2021. Identification of Cd-resistant microorganisms from heavy metal-contaminated soil and its potential in promoting the growth and Cd accumulation of bermudagrass. Environ Res. 200, 111730. 10.1016/j.envres.2021.111730

Xu, D.M., Fu, R.B., Liu, H.Q., 2021a. Current knowledge from heavy metal pollution in Chinese smelter contaminated soils, health risk implications and associated remediation progress in recent decades: A critical review. J. Clean. Prod. 286. 10.1016/j.jclepro.2020.124989

Xu, M., Huang, Q., Xiong, Z., Liao, H., Lv, Z., Chen, W., Luo, X., Hao, X., 2021b. Distinct Responses of Rare and Abundant Microbial Taxa to In Situ Chemical Stabilization of Cadmium-Contaminated Soil. mSystems. 6(5), e0104021. 10.1128/mSystems.01040-21

Yan, C., Wang, F., Geng, H., Liu, H., Pu, S., Tian, Z., Chen, H., Zhou, B., Yuan, R., Yao, J., 2020. Integrating high-throughput sequencing and metagenome analysis to reveal the characteristic and resistance mechanism of microbial community in metal contaminated sediments. Sci Total Environ. 707, 136116. 10.1016/j.scitotenv.2019.136116

Yun, S.W., Baveye, P.C., Kim, D.H., Kang, D.H., Lee, S.Y., Kong, M.J., Park, C.G., Kim, H.D., Son, J., Yu, C., 2018. Analysis of metal(loid)s contamination and their continuous input in soils around a zinc smelter: development of methodology and a case study in South Korea. Environ Pollut. 238, 140-149.

10.1016/j.envpol.2018.03.020

Zhang, B., Zhang, J., Liu, Y., Shi, P., Wei, G., 2018. Co-occurrence patterns of soybean rhizosphere microbiome at a continental scale. Soil Biology and Biochemistry. 118, 178-186. 10.1016/j.soilbio.2017.12.011

Zhang, K., Li, K., Tong, M., Xia, Y., Cui, Y., Liu, Z., Chen, Q., Li, Q., Hu, F., Yang, F., 2022a. Distribution Pattern and Influencing Factors of Heavy Metal Resistance Genes in the Yellow River Sediments of Henan Section. Int J Environ Res Public Health. 19(17). 10.3390/ijerph191710724

Zhang, M., Ye, J., He, J.S., Zhang, F., Ping, J., Qian, C., Wu, J., 2020. Visual detection for nucleic acid-based techniques as potential on-site detection methods. A review. Anal Chim Acta. 1099, 1-15. 10.1016/j.aca.2019.11.056

Zhang, M., Zhang, T., Zhou, L., Lou, W., Zeng, W., Liu, T., Yin, H., Liu, H., Liu, X., Mathivanan, K., Praburaman, L., Meng, D., 2022b. Soil microbial community assembly model in response to heavy metal pollution. Environ Res. 213, 113576. 10.1016/j.envres.2022.113576

Zhang, X., Chen, B., Yin, R., Xing, S., Fu, W., Wu, H., Hao, Z., Ma, Y., Zhang, X., 2022c. Long-term nickel contamination increased soil fungal diversity and altered fungal community structure and co-occurrence patterns in agricultural soils. J Hazard Mater. 436, 129113. 10.1016/j.jhazmat.2022.129113

Zhang, Z.F., Pan, J., Pan, Y.P., Li, M., 2021. Biogeography, Assembly Patterns, Driving Factors, and Interactions of Archaeal Community in Mangrove Sediments. mSystems. 6(3), e0138120. 10.1128/mSystems.01381-20

Zheng, W., Zhao, Z., Gong, Q., Zhai, B., Li, Z., 2018. Responses of fungal–bacterial community and network to organic inputs vary among different spatial habitats in soil. Soil Biology and Biochemistry. 125, 54-63. 10.1016/j.soilbio.2018.06.029

Zheng, W., Zhao, Z., Lv, F., Wang, R., Wang, Z., Zhao, Z., Li, Z., Zhai, B., 2021. Assembly of abundant and rare bacterial and fungal sub-communities in different soil aggregate sizes in an apple orchard treated with cover crop and fertilizer. Soil Biology and Biochemistry. 156. 10.1016/j.soilbio.2021.108222

Zhou, H., Gao, Y., Jia, X., Wang, M., Ding, J., Cheng, L., Bao, F., Wu, B., 2020. Network

analysis reveals the strengthening of microbial interaction in biological soil crust development in the Mu Us Sandy Land, northwestern China. Soil Biology and Biochemistry. 144. 10.1016/j.soilbio.2020.107782

Zhou, J.Z., Ning, D.L., 2017. Stochastic community assembly: does it matter in microbial ecology. Microbiol. Mol. Biol. Rev. 10.1128/MMBR

Zhou, L., Zhao, Z., Shao, L., Fang, S., Li, T., Gan, L., Guo, C., 2022. Predicting the abundance of metal resistance genes in subtropical estuaries using amplicon sequencing and machine learning. Ecotoxicol Environ Saf. 241, 113844. 10.1016/j.ecoenv.2022.113844

Zhu, X., Yao, J., Wang, F., Yuan, Z., Liu, J., Jordan, G., Knudsen, T.S., Avdalovic, J., 2018. Combined effects of antimony and sodium diethyldithiocarbamate on soil microbial activity and speciation change of heavy metals. Implications for contaminated lands hazardous material pollution in nonferrous metal mining areas. J Hazard Mater. 349, 160-167. 10.1016/j.jhazmat.2018.01.044

Zou, H.Y., He, L.Y., Gao, F.Z., Zhang, M., Chen, S., Wu, D.L., Liu, Y.S., He, L.X., Bai, H., Ying, G.G., 2021. Antibiotic resistance genes in surface water and groundwater from mining affected environments. Sci Total Environ. 772, 145516. 10.1016/j.scitotenv.2021.145516

Highlights

- The interaction between microbes, metal(loid)s, and soil properties was clarified.
- The links of fungal co-occurrence networks were higher than the bacterial networks.
- The keystone taxa were investigated in bacterial and fungal communities.
- Deterministic assemblies played a vital role in shaping the microbial community.

Figure captions

Fig. 1. Location of the abandoned non-ferrous metal(loid)s Huilong smelters (left) and distribution of sampling points (right), located in Zhongshan, Guangxi province, southwest China. The study area is delineated in red and different background colors represent different sites. The red dots represent the impact zone south of the smelter.

Fig. 2. Boxplots showing the soil total metal(loid)s concentrations in the non-ferrous metal(loid)s smelter and surrounding sites. Different lowercase letters in the boxplots indicate significant differences ($P < 0.05$) among the tested sites.

Fig. 3. Contributions of bioavailable metal(loid)s and edaphic parameters on bacterial beta diversity (NMDS1) in Huilong smelter and surrounding sites as predicted by the random forest model (A), and partial dependence of the predicted model (B), the black points and blue lines are the partial dependence data and trend, the red lines are the local polynomial regression fitting trends, with the 95% confidence limits (the gray band).

Fig. 4. Networks analysis between environmental variables and bacterial (A) and fungal (B) species among the top 500 abundant OTUs in the Huilong smelter regions. Edges are shown by strong correlations (Spearman $R > |0.6|$) and significant ($P < 0.05$). The nodes were colored by modularity class. The size of the node corresponds to the number of connections. The thickness of the edges corresponds to the strength of the correlation. Pink lines indicate positive interactions and green lines indicate negative interactions.

Fig. 5. Co-occurrence patterns of bacterial (A and B) and fungal (C and D) communities among the top 500 abundant OTUs in the Huilong regions. Edges are shown by strong correlations (Spearman $R > |0.6|$) and significant ($P < 0.05$). The nodes were colored by phylum (A and C) and modularity class (B and D). The thickness of the edges corresponds to the strength of the correlation. Light purple lines indicate positive interactions and green lines indicate negative interactions.

Fig. 6. Relative contributions of deterministic and stochastic processes for bacterial (A) and fungal (B) communities in the Huilong smelter and surrounding regions were determined using the null model framework.

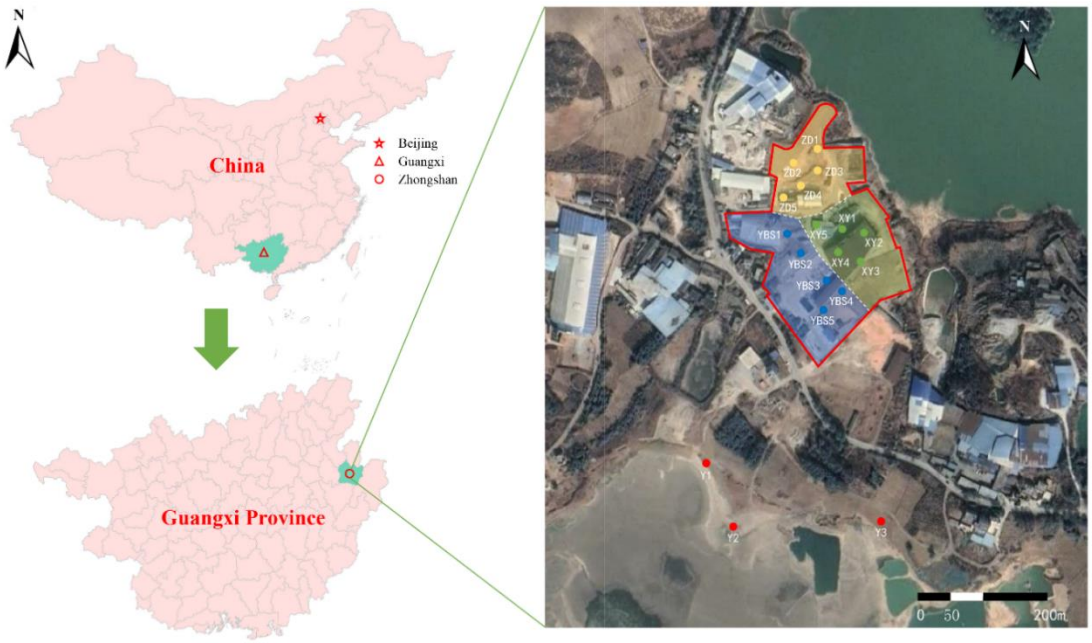

Fig. 1. Location of the abandoned non-ferrous metal(loid)s Huilong smelters (left) and distribution of sampling points (right), located in Zhongshan, Guangxi province, southwest China. The study area is delineated in red and different background colors represent different sites. The red dots represent the impact zone south of the smelter.

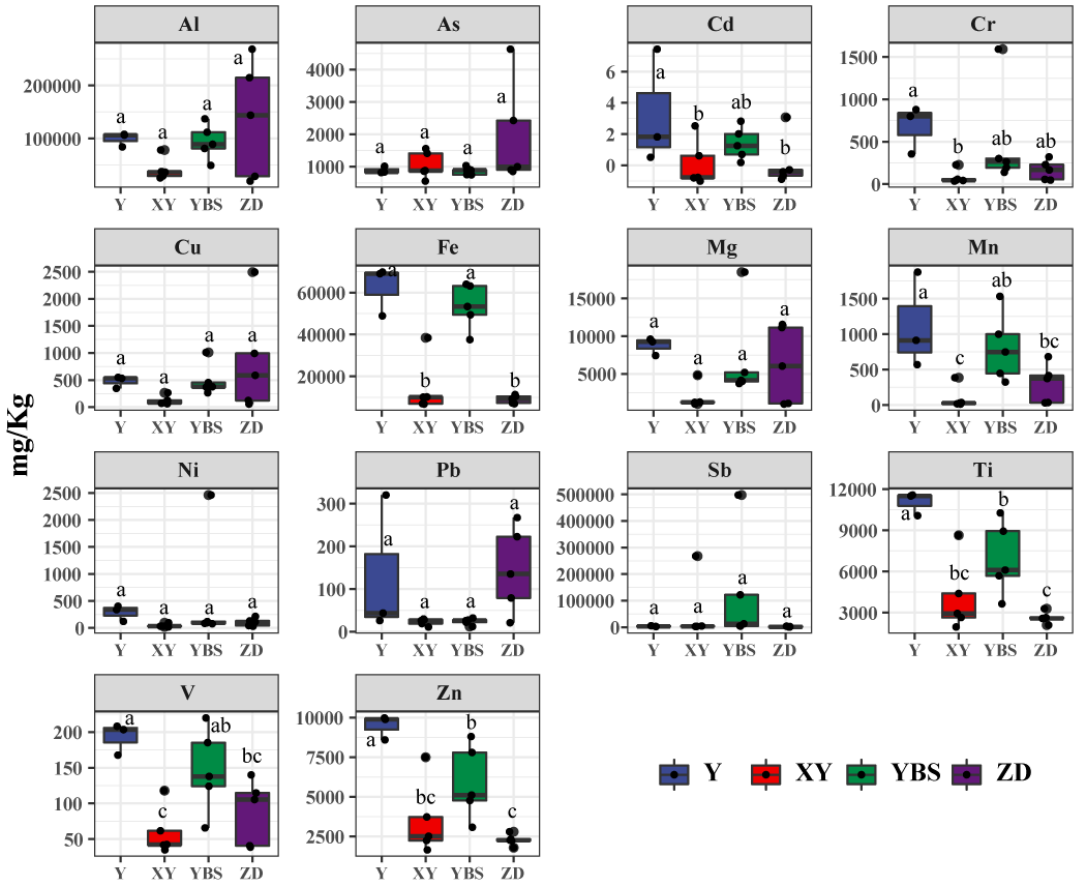

925

926 **Fig. 2.** Boxplots showing the soil total metal(loid)s concentrations in the non-ferrous
927 metal(loid)s smelter and surrounding sites. Different lowercase letters in the boxplots
928 indicate significant differences ($P < 0.05$) among the tested sites.

929

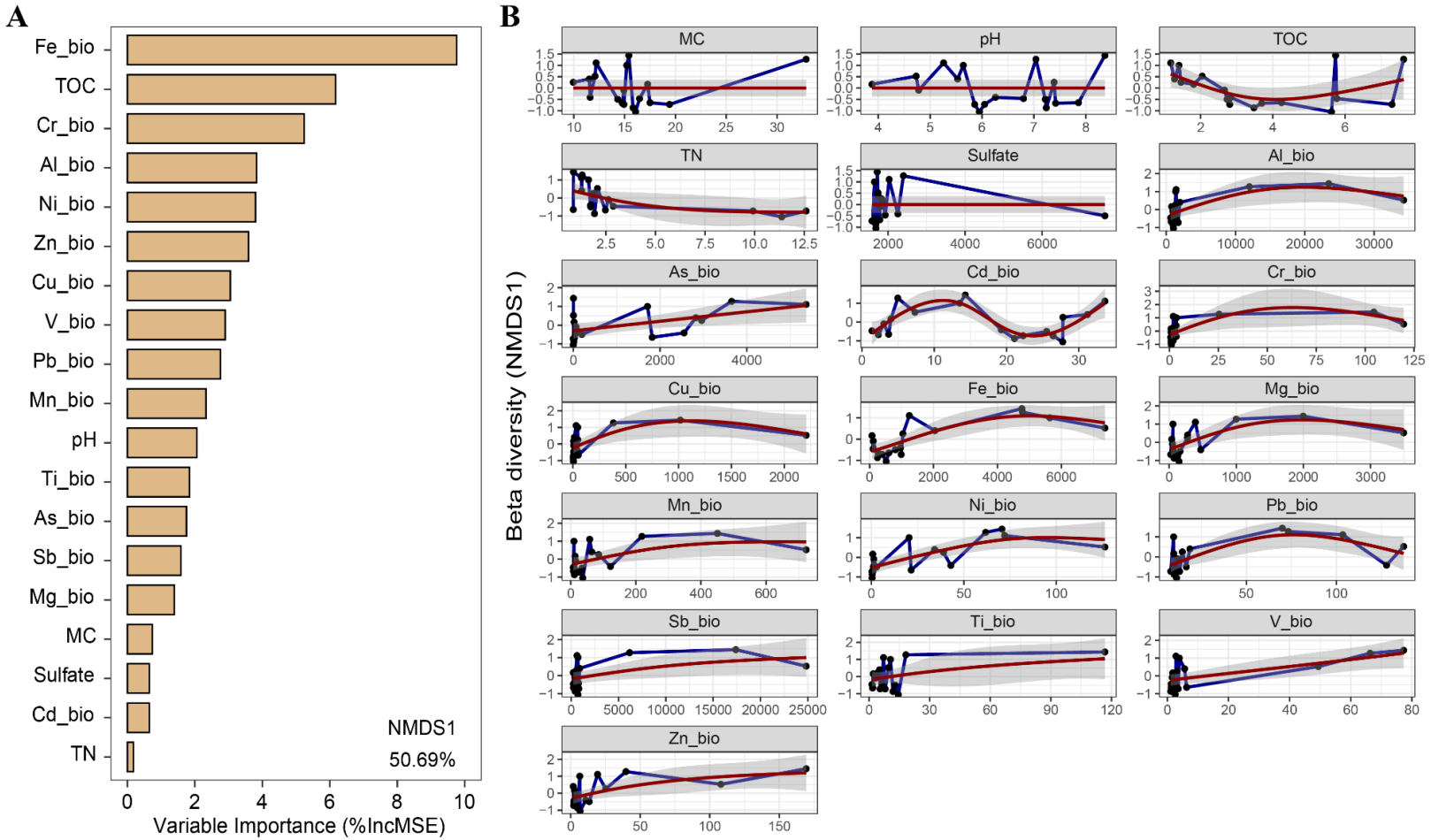

Fig. 3. Contributions of bioavailable metal(loid)s and edaphic parameters on bacterial beta diversity (NMDS1) in Huilong smelter and surrounding sites as predicted by the random forest model (A), and partial dependence of the predicted model (B), the black points and blue lines are the partial dependence data and trend, the red lines are the local polynomial regression fitting trends, with the 95% confidence limits (the gray band).

930

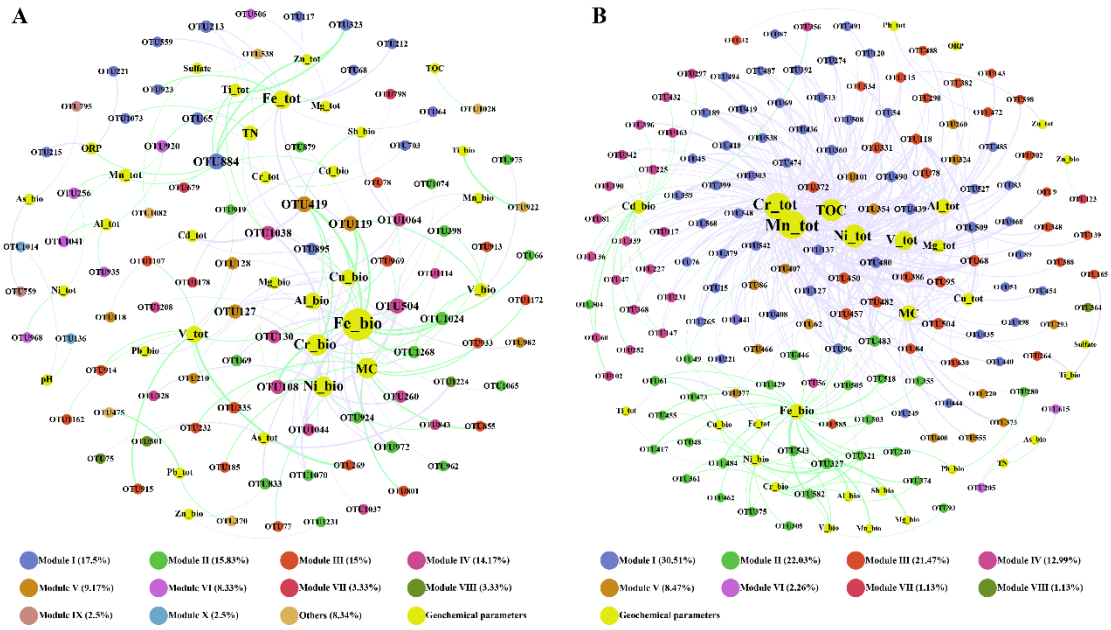

Fig. 4. Networks analysis between environmental variables and bacterial (A) and fungal (B) species among the top 500 abundant OTUs in the Huilong smelter regions. Edges are shown by strong correlations (Spearman $R > |0.6|$) and significant ($P < 0.05$). The nodes were colored by modularity class. The size of the node corresponds to the number of connections. The thickness of the edges corresponds to the strength of the correlation. Pink lines indicate positive interactions and green lines indicate negative interactions.

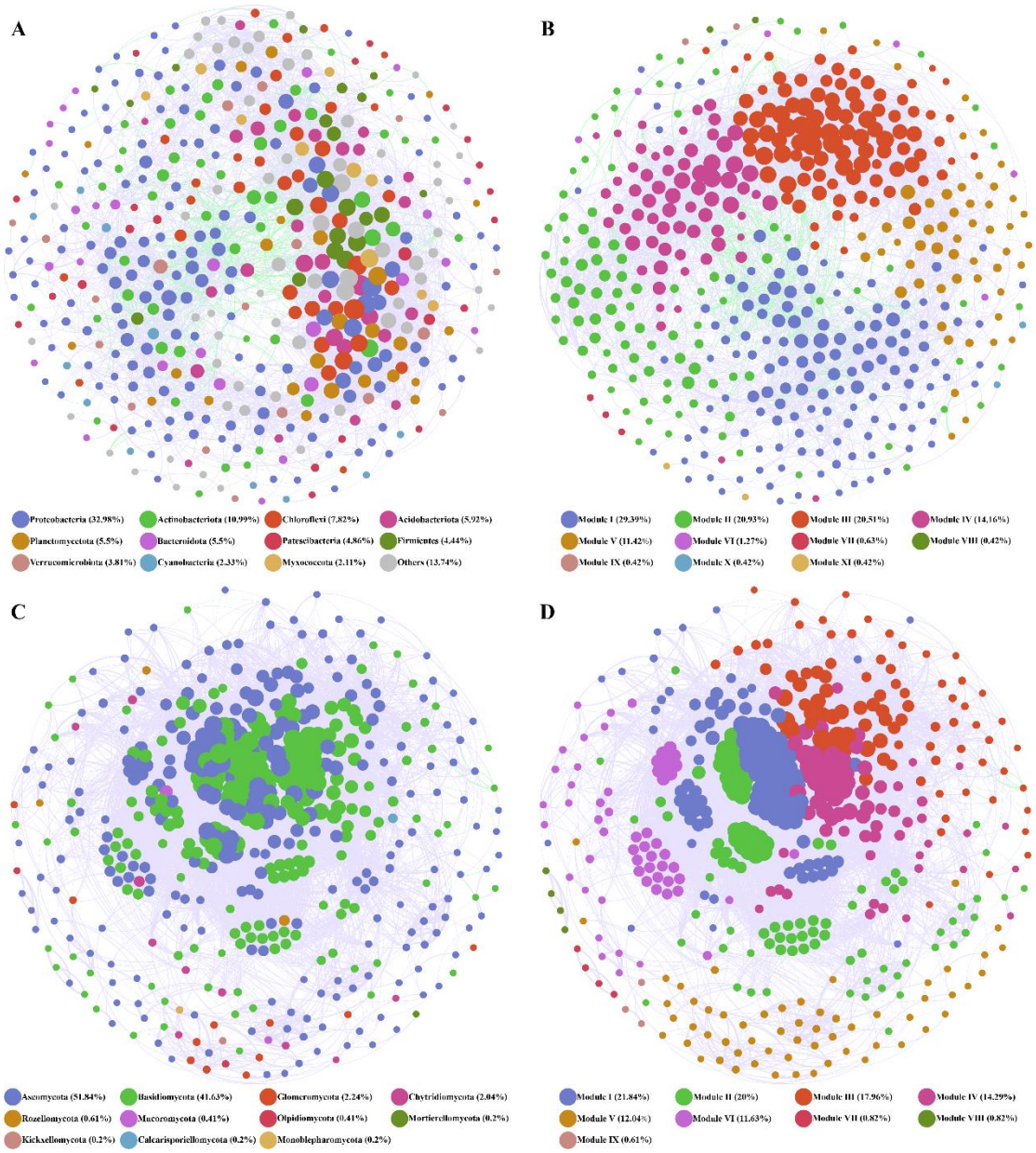

Fig. 5. Co-occurrence patterns of bacterial (A and B) and fungal (C and D) communities among the top 500 abundant OTUs in the Huilong regions. Edges are shown by strong correlations (Spearman $R > |0.6|$) and significant ($P < 0.05$). The nodes were colored by phylum (A and C) and modularity class (B and D). The thickness of the edges corresponds to the strength of the correlation. Light purple lines indicate positive interactions and green lines indicate negative interactions.

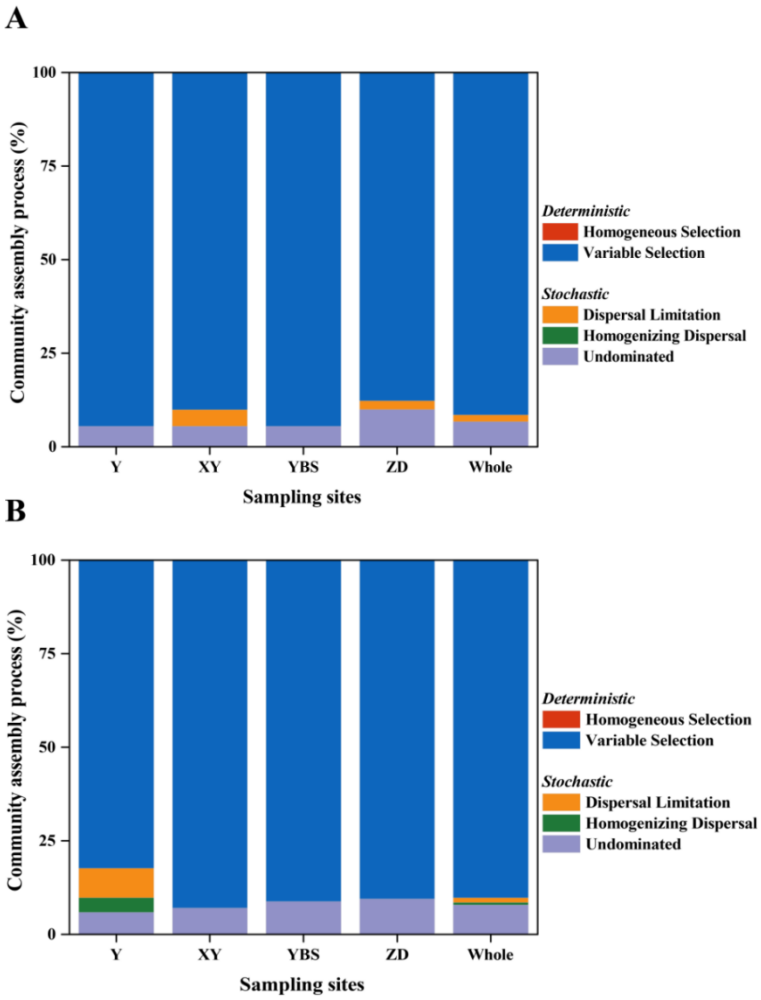

Fig. 6. Relative contributions of deterministic and stochastic processes for bacterial (A) and fungal (B) communities in the Huilong smelter and surrounding regions were determined using the null model framework.

Table 1. Topological characteristics of bacterial and fungal networks in Y, XY, YBS, and ZD sites.

Topological properties	Bacterial networks		Fungal networks	
	1*	2*	1*	2*
Nodes	473	120	490	177
Total links	5120	159	16559	520
Positive links	4706	82	16553	89
Negative links	414	77	6	431
Average degree	21.649	2.65	67.588	5.876
Clustering coefficient	0.433	0	0.584	0
Path distance	3.219	4.229	2.656	3.181
Density	0.046	0.022	0.138	0.033
Modularity	0.508	0.63	0.29	0.341

* abbreviations: 1, nodes of co-occurrence patterns were colored by phylum and modularity class in the bacterial or fungal communities network analysis; 2, networks analysis between environmental variables and bacterial or fungal species.